Available online at www.sciencedirect.com

ScienceDirect

Mendeleev Commun., 2024, **34**, 291–293

Mendeleev Communications

Canted antiferromagnetism in $Y_{2-x}Ca_xFeTaO_{7-\delta}$ solid solutions with a pyrochlore-like structure

Olga G. Ellert,[a] Elena F. Popova,[a] Denis I. Kirdyankin,[a] Vladimir K. Imshennik[b] and Anna V. Egorysheva*[a]

[a] *N. S. Kurnakov Institute of General and Inorganic Chemistry, Russian Academy of Sciences, 119991 Moscow, Russian Federation. E-mail: anna_egorysheva@rambler.ru*

[b] *N. N. Semenov Federal Research Center for Chemical Physics, Russian Academy of Sciences, 119991 Moscow, Russian Federation*

DOI: 10.1016/j.mencom.2024.02.043

The existence of $Y_{2-x}Ca_xFeTaO_{7-\delta}$ solid solutions (x = = 0–0.075) with a pyrochlore-like layered structure was established. The appearance of the magnetic properties characteristic for canted antiferromagnets was observed as a result of structure distortions (space group $R\bar{3} \rightarrow$ space group $P3_121$) associated with a change of composition. $Y_{2-x}Ca_xFeTaO_{7-\delta}$ exhibits ferromagnetic properties already at 300 K.

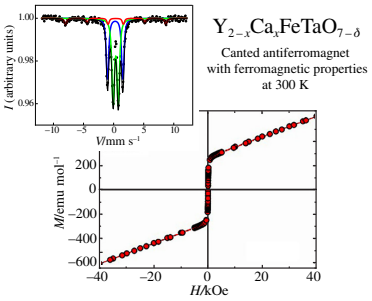

Keywords: Y_2FeTaO_7, Ca^{2+}, solid solutions, canted antiferromagnets, spin-reorientation transition, Dzyaloshinskii–Moriya interaction.

Antiferromagnetic spintronics is a promising field of next-generation electronics, since it can potentially provide information transmission without dissipation due to the transfer of spin angular momentum.[1] Both collinear and non-collinear antiferromagnets can efficiently generate spin pumping, significantly increasing the operating frequency of spintronic devices.[2] The use of canted antiferromagnets with the Dzyaloshinsky-Moriya interaction, in which ferromagnetic and antiferromagnetic properties coexist, opens up new ways of creating efficient generators, detectors and transmitters of spin currents.[3–6]

Previously, we detected ferromagnetic (FM) properties at room temperature and magnetic behavior characteristic of canted antiferromagnets with T_N > 300 K in solid solutions based on Y_2FeTaO_7 obtained by means of iso- or heterovalent substitution: $Y_{1.8}Fe_{1.2}TaO_7$, $Y_2Fe_{0.55}Mg_{0.3}Ta_{1.15}O_7$, $Y_2Fe_{0.625}Mg_{0.3}Ta_{1.075}O_7$, $Y_2Fe_{0.7}Mg_{0.3}TaO_7$, $Y_2Fe_{0.7}Mg_{0.2}Ta_{1.1}O_7$, $Y_2Fe_{0.85}Mg_{0.15}TaO_7$, $Y_{1.85}Mg_{0.15}Fe_{0.925}Ta_{1.075}O_7$, and $Y_{1.85}Mg_{0.15}FeTaO_7$.[7,8] Unlike of the pyrochlore-like layered compound Y_2FeTaO_7 (space group $R\bar{3}$) the crystal lattices of noted above solid solutions are described by space group $P3_121$. The structural changes observed in these solid solutions give rise to the appearance of magnetic properties that are not characteristic of stoichiometric compounds. For $Y_{1.8}Fe_{1.2}TaO_7$ and Mg-containing solid solutions rapid saturation of magnetization (M) in small fields and further linear increase in magnetization with increaseing applied magnetic field and $M(H)$ hysteresis at 300 and 2.3 K were observed.[7,8] Weak ferromagnetism found in the structures under discussion is associated with the appearance of spontaneous magnetization due to the significant ferromagnetic (FM) component of Fe^{3+} spin arrangement with a noticeable canting in compounds with predominantly AFM interactions.[9,10] It has been shown that three magnetic phase transitions occur in solid solutions containing Mg, namely, antiferromagnetic transitions at T_N > 300 K, transitions caused by spin reorientation with transition temperatures in the range T_{tr} ~ 137–268 K. At the same time, in the samples with a sufficiently large Fe content a spin-glass transition occurs at extremely low temperatures due to frustration existing in the magnetic subsystem.[8,11]

This work is a continuation of the study of canted antiferromagnets with a pyrochlore-like structure. The effect of heterovalent substitution of Y^{3+} for a cation with a large ionic radius Ca^{2+} on the magnetic properties has been studied.

The synthesis of the $Y_{2-x}Ca_xFeTaO_{7-\delta}$ samples was carried out by sol–gel method similar according to procedure described elsewhere.[8] The solid solution was found to exist in a narrow region x = 0–0.075. However, even such a slight change in composition gives rise to structural distortions (space group $R\bar{3} \rightarrow$ space group $P3_121$), similar to those observed with the substitution of Mg^{2+}.[8] The structure of $Y_{2-x}Ca_xFeTaO_{7-\delta}$ is a

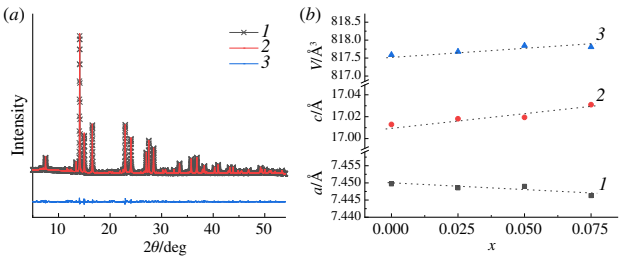

Figure 1 (*a*) Experimental (*1*) and theoretical (*2*) X-ray patterns of $Y_{1.925}Ca_{0.075}FeTaO_7$ and the difference (*3*) for the model of space group $P3_121$. (*b*) Dependence of the structural parameters (*1*) a and (*2*) c, and also (*3*) the unit cell volume on the value of x in $Y_{2-x}Ca_xFeTaO_{7-\delta}$ for space group $P3_121$.

layer of Fe/Ta–O polyhedra, between which Y^{3+} ions are situated.† The calculation using the Le Bel method showed that the entry of Ca^{2+} is accompanied by a decrease in parameter *a*, determined by the geometry of the Fe/Ta–O polyhedra layer, and an increase in parameter *c*, depending on the distance between these layers (Figure 1 and Table 1). An important feature of this structure is the existence of 3 nonequivalent sites in the layer of Fe/Ta–O polyhedra, according to which iron ions can be distributed, instead of 2 sites in the parent structure of Y_2FeTaO_7. The appearance of the third site for iron ions is proved by Mössbauer (MB) spectroscopy [Figure 2(*a*) and Table 2].‡ The MB spectra of $Y_{1.925}Ca_{0.075}FeTaO_7$ is described by two doublets and one sextet that are characteristic for the $Y_2Fe_{0.7}Mg_{0.3}TaO_7$ and $Y_{1.85}Mg_{0.15}FeTaO_7$ spectra studied earlier.[8] The parameters of one doublet are typical for octahedrically coordinated Fe^{3+} ions in the high-spin state, and the other corresponds to an eight-coordinated iron ion in the $Fe^{3+/4+}$ mixed-charge state.[7,8] The magnetic sextet with the hyperfine magnetic field value H_{hf} = 51.4 T corresponds to the third site and points to the existence of the magnetic ordering (spontaneous magnetization) in $Y_{2-x}Ca_xFeTaO_{7-\delta}$ already at room temperature.

Magnetic properties of $Y_{2-x}Ca_xFeTaO_{7-\delta}$ solid solutions were studied using $Y_{1.975}Ca_{0.025}FeTaO_7$ and $Y_{1.925}Ca_{0.075}FeTaO_7$ samples as an example.§ For these samples the temperature dependence of magnetization $M(T)$ in the magnetic field H = = 5000 Oe increases smoothly while temperature decreases; however, in $Y_{1.925}Ca_{0.075}FeTaO_7$, the magnetization at 300 K is

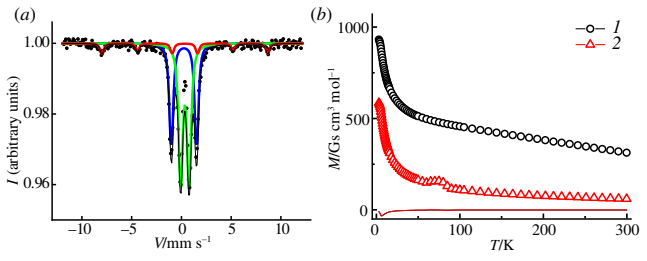

Figure 2 (*a*) Mössbauer spectra of $Y_{1.925}Ca_{0.075}FeTaO_7$ at T = 300 K. (*b*) Temperature dependences of magnetization $M(T)$ of samples (*1*) $Y_{1.975}Ca_{0.025}FeTaO_7$ and (*2*) $Y_{1.925}Ca_{0.075}FeTaO_7$ at H = 5000 Oe.

Table 1 The results of the refinement of the $Y_{2-x}Ca_xFeTaO_{7-\delta}$ structure by the Le Bel method for the model of space group $P3_121$.

Substitution degree, *x*	*a*/Å	*c*/Å	*V*/Å^3	GOF
0.025	7.4486(1)	17.0181(3)	817.68(2)	1.96
0.05	7.4490(1)	17.0194(2)	817.846(16)	1.53
0.075	7.4463(1)	17.0310(3)	817.810(17)	1.55

Table 2 Mössbauer characteristics of $Y_{1.925}Ca_{0.075}FeTaO_7$ (space group $P3_121$) at T = 300 K.

Fe species	CN	δ [a]	Δ [b]	Γ [c]	H_{hf} [d]	A [e]
		±0.03/mm s^{-1}			±0.5/T	±0.05
$Fe^{3+\delta}$– paramagnetic[e]	8	0.23	2.54	0.40	–	0.38
Fe^{3+} – magnetic	6	0.35	0.13	0.36	51.4	0.09
Fe^{3+} – paramagnetic	6	0.36	0.90	0.41	–	0.53

[a] δ is the isomer shift relative to α-Fe, [b] Δ is the quadrupole splitting, [c] Γ is the line width, [d] H_{hf} is the hyperfine field at the ^{57}Fe nucleus, [e] A is the relative content, and $Fe^{3+\delta}$ is the mixed charge state $Fe^{3+/4+}$.

† The measurements were carried out at the RSA station of the UNU 'Kurchatov synchrotron radiation source'.

‡ Mössbauer spectra were measured on a Wesel spectrometer using a ^{57}Co (Rh) radiation source with an activity of 1.1 GBq.

§ DC and AC magnetization measurements were made using a Quantum Design PPMS-9 system.

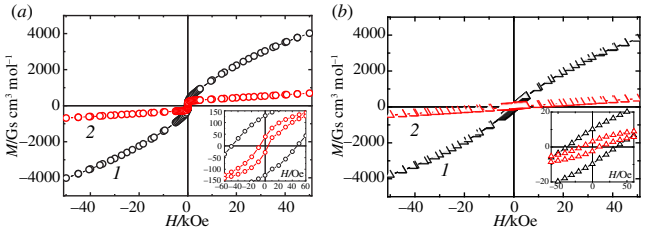

Figure 3 Field dependences of the magnetization of samples (*a*) $Y_{1.975}Ca_{0.025}FeTaO_7$ and (*b*) $Y_{1.925}Ca_{0.075}FeTaO_7$ at temperatures of (*1*) 2.3 and (*2*) 300 K. Insets: $M(H)$ in a low field.

about an order of magnitude lower than for $Y_{1.975}Ca_{0.025}FeTaO_7$. At T_{tr} = 71 K, a peak is observed which can be attributed to the magnetic transition of the atiferromagnetic (AFM) type [Figure 2(*b*)]. This transition is confirmed on the differential curve dM/dT (data are no provided), and at the lowest temperatures, the transition, most likely, to a spin glass (SG) state is registered [Figure 2(*b*)]. The above data indicate the ferrimagnetic behavior of $Y_{2-x}Ca_xFeTaO_{7-\delta}$ which is confirmed by the characteristic field dependences of $M(H)$.

Indeed, the $M(H)$ curves for $Y_{1.975}Ca_{0.025}FeTaO_7$ and $Y_{1.925}Ca_{0.075}FeTaO_7$ are characteristic of ferrimagnets or canted antiferromagnets. We observe rapid magnetization in small fields at both 2.3 and 300 K, hysteresis at 300 and 2.3 K, small values of residual magnetization and linear AFM contribution, while $M(H)$ does not reach saturation up to 5 T [Figure 3(*a*),(*b*) and Table 3]. The similar magnetic behavior was detected for Mg-containing solid solutions.[8] It is clearly seen that in $Y_{1.925}Ca_{0.075}FeTaO_7$ the contribution of FM interactions is significantly less [Figure 3(*a*),(*b*)], which confirms the $M(T)$ data in the magnetic field H = 5000 Oe [Figure 2(*b*)]. Probably, an increase in the number of large Ca^{+2} ions at the Y^{3+} site causes additional structural distortions in the layers of the (Fe/Ta)O_6 octahedra, which can give rise to a change in the spin canting angle and a decrease in the total magnetization compared to the $Y_{1.975}Ca_{0.025}FeTaO_7$ sample.

Measurements in small fields, H = 100 Oe, show a wide maximum on the ZFC curve in $Y_{1.975}Ca_{0.025}FeTaO_7$ [Figure 4(*a*)], which, by analogy with Mg-containing samples, indicates a possible transition due to a reorientation of spins like in a number of other canted antiferromagnets.[12–16] The differential curve dM/dT [Figure 4(*b*)] and also the magnetization plateau observed at lower temperatures and associated with rapid magnetization in small fields confirm the transition at T_{tr} = 131 K. On the contrary, for $Y_{1.925}Ca_{0.075}FeTaO_7$, the transition, T_{tr} = 71 K, detected at 5000 Oe, is scarcely distinguishable in a weak magnetic field of 100 Oe [Figure 4(*a*)]. At the same time, this transition is 'drawn' on the differential curve ZFC in the region of 71 K and can also be caused by the reorientation of spins [Figure 4(*b*)]. Measurements in an alternating field confirm the competition of AFM and FM magnetic exchange interactions. As a result, frustration of the spin system causes transitions into SG in both samples at T_g = 4.3 K [Figure 5(*a*),(*b*)].

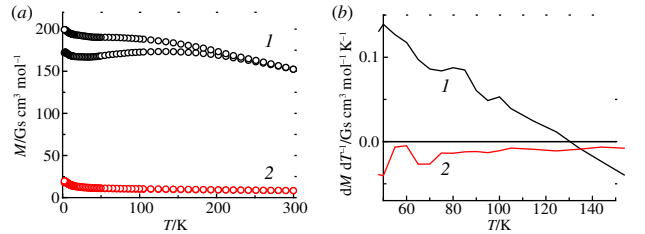

Figure 4 (*a*) Magnetic behavior $M(T)$ of samples (*1*) $Y_{1.975}Ca_{0.025}FeTaO_7$ and (*2*) $Y_{1.925}Ca_{0.075}FeTaO_7$ in ZFC–FC modes at H = 100 Oe and (*b*) dM/d$T(T)$ differential curves.

Table 3 Experimental and calculated magnetic characteristics of $Y_{1.975}Ca_{0.025}FeTaO_7$ and $Y_{1.925}Ca_{0.075}FeTaO_7$.

Sample	H_c[a]/Oe		M_R[b]/Gs cm^3 mol^{-1}		μ_s/μ_B[c]		T_g[d]/K	T_{tr}[e]/K
	2.3 K	300 K	2.3 K	300 K	2.3 K	300 K		
$Y_{1.975}Ca_{0.025}FeTaO_7$	49 ± 2	8 ± 2	128 ± 0.5	39 ± 0.5	0.03 ± 0.01	0.03 ± 0.01	4.3 ± 0.5	130 ± 2
$Y_{1.925}Ca_{0.075}FeTaO_7$	37 ± 2	16 ± 2	10 ± 0.5	3 ± 0.5	0.02 ± 0.01	0 ± 0.01	4.3 ± 0.5	71 ± 2

[a] Coercive force. [b] Spontaneous magnetization. [c] Calculated saturation moment. [d] SG transition temperature. [e] T_{tr} is the transition temperature from dM/d$T(T)$ of ZFC.

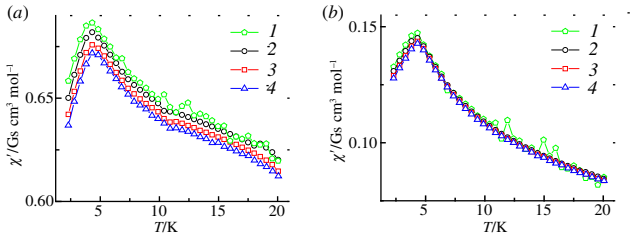

Figure 5 AC magnetization $\chi'(T)$ of samples (*a*) $Y_{1.975}Ca_{0.025}FeTaO_7$ and (*b*) $Y_{1.925}Ca_{0.075}FeTaO_7$ at (*1*) 100, (*2*) 1000, (3) 5000 and (*4*) 10000 Hz.

Thus, the entry of Ca^{2+} ions into the crystal lattice of Y_2FeTaO_7 leads to a structural transition (spatial group $R\bar{3} \rightarrow$ spatial group $P3_121$) similar to what we found earlier in Mg-containing solid solutions.[8] As a result, Fe^{3+} magnetic ions are distributed over three nonequivalent sites. Magnetic properties in such a spin system are described by antiferromagnetic exchange interactions between Fe^{3+} in neighboring octahedra and weak ferromagnetism arising from the canting of spins as well. In all studied solid solutions spontaneous magnetization is observed already at room temperature, as well as magnetization isotherms $M(H)$ at 300 and 2.3 K, which are characteristic of canted antiferromagnets. Three magnetic phase transitions are recorded in each sample, namely, an antiferromagnetic one at $T_N > 300$ K, a transition which is due to reorientation of spins, and also, with a sufficiently large iron content, a transition to a spin glass state at $T_g \leqslant 4.3$ K. The obtained correlations of structure/magnetic properties allow us to modify the pyrochlore-like solid solutions based on Y_2FeTaO_7 to create new promising canted antiferromagnets for spintronics .

The research was carried out with the financial support from the Russian Science Foundation grant no. 22-23-00365.

References

1 V. Baltz, A. Manchon, M. Tsoi, T. Moriyama, T. Ono and Y. Tserkovnyak, *Rev. Mod. Phys*., 2018, **90**, 015005.
2 T. Jungwirth, X. Marti, P. Wadley and J. Wunderlich, *Nat. Nanotechnol.*, 2016, **11**, 231.
3 I. Boventer, H. T. Simensen, A. Anane, M. Kläui, A. Brataas and R. Lebrun, *Phys. Rev. Lett*., 2021, **126**, 187201.
4 P. Němec, M. Fiebig, T. Kampfrath and A. V. Kimel, *Nat. Phys*., 2018, **14**, 229.
5 J. Han, R. Cheng, L. Liu, H. Ohno and S. Fukami, *Nat. Mater.*, 2023, **22**, 684.
6 P. Stremoukhov, A. Safin, M. Logunov, S. Nikitov and A. Kirilyuk, *J. Appl. Phys.*, 2019, **125**, 223903.
7 A. V. Egorysheva, O. G. Ellert, E. F. Popova, D. I. Kirdyankin and Yu. V. Maksimov, *Mendeleev Commun.*, 2023, **33**, 519.
8 O. G. Ellert, E. F. Popova, D. I. Kirdyankin, V. K. Imshennik, E. S. Kulikova and A. V. Egorysheva, *Russ. J. Inorg. Chem.*, 2023, **68**, 1325 (*Zh. Neorg. Khim.*, 2023, **68**, 1339).
9 A. S. Moskvin and S.-L. Drechsler, *Phys. Rev. B: Condens. Matter Mater. Phys.*, 2008, **78**, 024102.
10 T. Yamaguchi, *J. Phys. Chem. Solids*, 1974, **35**, 479.
11 O. G. Ellert and A. V. Egorysheva, in *Pyrochlore Ceramics: Properties, Processing, and Applications*, ed. A. Chowdhury, Elsevier, Amsterdam, 2022, pp. 315–338.
12 F. J. Morin, *Phys. Rev*., 1950, **78**, 819.
13 L. T. Tsymbal, V. I. Kamenev, Ya. B. Bazaliy, D. A. Khara and P. E. Wigen, *Phys. Rev. B*, 2005, **72**, 052413.
14 H. Pinto, G. Shachar, H. Shaked and S. Shtrikman, *Phys. Rev. B*, 1971, **3**, 3861.
15 V. D. Doroshev, A. S. Kharnachev, N. M. Kovtun, E. E. Soloviev, A. Ya. Chervonenkis and A. A. Shemyakov, *Phys. Status Solidi B*, 1972, **51**, 31.
16 S. Bhattacharjee, A. Senyshyn, H. Fuess and D. Pandey, *Phys. Rev. B*, 2013, **87**, 054417.

Received: 23rd November 2023; Com. 23/7314